Influencing factor analysis of the Principal Component Analysis for the characterization and restoration of phase aberrations due to atmospheric turbulence

Jiangpuzhen Wang [1,2,3]- ZhiQiang Wang[1] [1,3,a,*] - Jinghui Zhang [1,4]- Chunhong Qiao[2] [1,4] and Chengyu Fan [1,3,b,*]

1 Key Laboratory of Atmospheric Optics, Anhui Institute of Optics and Fine Mechanics, HFIPS, Chinese Academy of Sciences, Hefei 230031, China

2 Science Island Branch of Graduate School, University of Science and Technology of China, Hefei 230026, China

3 Nanhu Laser Laboratory, National University of Defense Technology, Changsha 410073, China

4 State Key Laboratory of Laser Interaction with Matter, Anhui Institute of Optics and Fine Mechanics, HFIPS, Chinese Academy of Sciences, Hefei 230031, China

a. zqwang@aiofm.ac.cn;

b. cyfan@aiofm.ac.cn.

Abstract: Restoration of phase aberrations is crucial for addressing atmospheric turbulence involved light propagation. Traditional Zernike polynomials (ZPs) restoration algorithms often encounter challenges related to high computational complexity and insufficient capture of high-frequency phase aberration components, so we proposed Principal Component Analysis based method for representation of phase aberrations. This paper discusses the factors that influence the accuracy of restoration using Principal Components (PCs), mainly the size of sample space and sampling interval of D/r_0, which is used to characterize the strength with r_0 being the atmospheric coherence length and D being the pupil diameter, on the basis of characterizing phase aberrations by PCs. The experimental results show that: a larger D/r_0 sampling interval can ensure the generalization ability and robustness of the principal components in the case of a limited amount of original data, which can help to quickly achieve high-precision deployment of the model in practical applications. In the environment of

[1] This work has been supported by the National Natural Science Foundation of China (No: 12273084);

[2] This work has also been supported by Science and Technology Innovation Fund for Key Laboratories of the Chinese Academy of Sciences (No: CXJJ-225028).

relatively strong turbulence in the test set of D/r_0 = 24, the use of 34 terms of PCs can improve the corrected Strehl ratio (SR) from 0.007 to 0.1585, while the Strehl ratio of the light spot after restoration using 34 terms of ZPs is only 0.0215, which has almost no correction effect. The results indicate that PCs can be served as a better alternative in representing and restoring the characteristics of atmospheric turbulence induced phase aberrations. These findings pave a way to use PCs of phase aberrations with less terms than traditional ZPs to achieve data dimensionality reduction, and offer a reference to accelerate and stabilize the model based and deep learning based adaptive optics correction.

Key words: phase aberration; atmospheric turbulence; principal component analysis; Zernike polynomials

基于主成分分析法的大气湍流相位畸变表征和还原影响因素分析

王姜菩真[1,2,3]，王志强[1,3,*]，张京会[1,4]，乔春红[1,4]，范承玉[1,3,*]

([1]中国科学院合肥物质科学研究院安徽光学精密机械研究所中国科学院大气光学重点实验室，安徽 合肥 230031
[2]中国科学技术大学研究生院科学岛分院，安徽 合肥 230026
[3]南湖之光实验室，中国人民解放军国防科技大学，湖南 长沙 410073
[4]激光与物质相互作用全国重点实验室，中国科学院合肥物质科学研究院安徽光机所，安徽 合肥 230031)

摘 要：为了有效表征、还原大气湍流造成的相位畸变，解决传统Zernike多项式方法引起的相位还原高频信息不足问题，提出了基于主成分分析法的畸变相位特征表征、还原方法，对可能影响主成分精度从而影响还原效果的因素进行研究。首先建立了几组包含满足Von-Karman功率谱的畸变相位的原始数据集，几组数据集样本数量不等，并生成了D/r_0采样间隔分别为1和10的样本空间，D/r_0用于描述湍流强度，其中r_0是大气相干长度，D是光瞳直径。接着建立了不同湍流强度下畸变相位的测试集数据。之后从不同原始数据集中提取对应的主成分，并分别使用相同项数的主成分与Zernike多项式对同一组测试集畸变相位进行还原。最终对比还原结果，分析原始数据样本量和D/r_0采样间隔对主成分精度的影响。实验结果表明结果：更大的D/r_0采样间隔可以在原始数据量有限的情况下保证主成分的泛化能力和鲁棒性，从而帮助实际应用中快速实现模型的高精度部署；在测试集D/r_0=24的相对湍流较强的环境下，使用34阶主成分可以将校正后光斑Strehl比从原始的0.007提升至0.1585，而同样使用34阶Zernike还原后的光斑Strehl比仅为0.0215，几乎没有校正效果。可以看出基于主成分分析法的大气湍流相位畸变表征和还原方法优于Zernike多项式，可以为基于模型和深度学习的自适应光学校正提供参考。

关键词：相位畸变；大气湍流；主成分分析法；Zernike 多项式

中图分类号：TP394.1；TH691.9　　文献标识码：A

1. Introduction

Atmospheric turbulence can affect the quality of light waves and then impact the clarity and resolution of astronomical observations and the transmission of free-space optical communications [1,2]. Adaptive optics technology was therefore proposed to correct phase aberrations caused by atmospheric turbulence using efficient wavefront sensing [3,4].

Both traditional Shack–Hartmann wavefront sensor and the shearing interferometer have problems and thus can't restore phase distortion very well. The Shack–Hartmann wavefront sensor can only measure the phase aberration with limited spatial resolution because of the sub-aperture constriction [5,6]. And the shearing interferometer splits the beam into two wavefronts, which lower the light energy utilization efficiency and subsequently reduce the accuracy of wavefront sensing [7,8]. In recent years, image-based wavefront sensing has gained attention. With the help of deep learning (DL), wavefront reconstruction is now much more efficient and accurate [9-12]. Paine et al [13] predicted Zernike polynomials (ZPs) coefficients from a computational simulated point spread function (PSF) using convolutional neural network (CNN) for the reconstruction of wavefront in 2018. Nishikazi et al [14] experimentally verified the effectiveness of CNN in predicting coefficients of ZPs and estimating wavefront aberrations in 2019. Ge et al [15] further used a DL network to achieve high-precision mapping of phase features to wavefront aberrations in phase reconstruction in 2024.

Most image-based wavefront sensing methods use ZPs, a classic way to represent phase aberrations, as mentioned above. The higher the term of ZPs used, the more high-frequency components captured, and the more accurate the restoration of phase aberrations [16]. However, using more ZPs makes the computer work harder, which makes prediction less accurate by CNN model [17], while using fewer ZPs reduces the generalization ability of the model to deal with complex environments such as strong

turbulence.

Currently, the statistical Principal Component Analysis (PCA) method is becoming popular. PCA can identify the most dominated features from a large dataset. Over the past few years researchers have successfully applied PCA to reduce speckle noise [18], denoise meteorological echoes [19], and combine with neural network to correct non-common path aberrations [20].

Inspired by the success implementation of using PCA, we had performed PCA on representation of phase aberrations caused by atmospheric turbulence and proved its validity. In this work, we discussed the factors affecting the restoration accuracy by principal components (PCs), mainly the size of sample space and sampling interval of D/r_0 on the basis of characterizing phase aberrations by PCs. In section 2, we provide a basic overview of the method used in the paper, and section 3 introduces the simulation process. We verify and compare the representation and restoration performance of PCA method with the traditional ZPs method in section 4. Our analysis proved that the PCA method evidently outperforms traditional ZPs across varying atmospheric turbulence strength, especially in challenging situations such as strong turbulence, providing a statistical reference for data acquisition for PCs model deployment in real applications.

2. Methods

To simulate atmospheric turbulence accurately, we create a phase screen data set that satisfies the modified Von Karman power spectrum using Fast Fourier Transform [21], and the inner and outer scale of atmospheric turbulence are set as 0.005m and 10m. According to Noll [22], the phase aberration $W(\rho,\theta)$ can be represented as a combination of ZP $Z_j(\rho,\theta)$ with coefficients a_j. This paper ignores the first three terms of ZPs, which does not change the morphology of the aberration, and focuses on the aberration above the 4th term: defocus. As ZP patterns are generally grouped in terms of spherical aberration, it is generally accepted that aberration patterns prior to the

tertiary Spherical aberration carry more weight and the use of more terms increases the computational burden, but the improvement to aberration restoration is small. So, we used 4th to 37th ZPs (tertiary Spherical aberration) to fit the original phase aberration and set the piston, x tilt, and y tilt terms to 0 to generate a new phase aberration dataset, as shown in the following expression:

$$W_1(\rho,\theta)=\sum_{j=4}^{37}a_j Z_j(\rho,\theta), \tag{1}$$

Where ρ and θ are the radial and azimuthal variables in a polar coordinate. ZPs have a specific pattern for each term, with more information in higher terms. More terms allow the phase aberration to be restored more finely, but it is slower and less efficient. A few terms are therefore often used but higher frequencies are often missed. Then, we propose PCA method, a useful statistical tool for reducing multiple complex variables, to represent and restore the phase aberrations. The old variables are combined to form new variables as:

$$y_i = V' x_i, \tag{2}$$

where $y_i=(y_{1i},y_{2i},\cdots,y_{ni})'$ is the new variable, $x_i=(x_{1i},x_{2i},\cdots,x_{ni})'$ is the original variable. This approach keeps the information in both lower and higher-term components in each new single mode. The first m new variables with the highest variance, i.e., the PCs, are selected to distill the essence of the original dataset. This summary shows the main features of the original data and reduces the number of dimensions. To be consistent with Eq.(1) above, the representation of the phase aberration fitted using the first 34 terms of PCs is shown below:

$$W_2(\rho,\theta)=\sum_{j=1}^{34}[(C^T)^{-1}\times PC_j], \tag{3}$$

where C is the transformation matrix of PCA, and PC_j is the j^{th} PC term. To analyze the validity of PCA in different conditions, we need to create datasets that show

different levels of turbulence. Based Lane's derivation [23], D/r_0 is used to characterize the strength with r_0 being the atmospheric coherence length and D being the pupil diameter. The numerical interval is D/r_0 from 1 to 30. Where, 1-10 is relatively weak turbulence, 10-20 is medium and 20-30 is relatively strong. Further, the Strehl ratio (SR) of the PSF is used to evaluate the effectiveness of phase restoration by performing a fast Fourier transform on the residual phase aberration.

3. Simulation

This paper focuses on the analysis of the influencing factors of the accuracy of PCs restoration of phase aberration, which are: size of the sample space of the original phase data, and the sampling interval of D/r_0. In order to conduct a more comprehensive analysis of the restoration effectiveness of PCs in different propagation conditions, generating phase datasets that can encompass different turbulence strength is necessary.

The simulation was performed according to the following steps:

(1) Generate the original sample space containing N distorted phases randomly, then perform a PCA on the base data to generate the PCs respectively. We chose N = 5000, 10000 and 30000.

(2) For the equivalent size of sample space, generate two sample spaces with different D/r_0 sampling intervals, average distribution between 1-30 as space *A*, and D/r_0=5, 15, and 25 as representative values of weak, medium and strong turbulence, respectively, as space *B*, and perform a PCA on datasets *A* and *B* to extract corresponding PCs.

(3) Restore the phase aberrations of the test set under different turbulence strength using 8,19,34 terms of ZPs and PCs obtained from different sample spaces. The terms employed are based on the Zernike primary, secondary and tertiary spherical aberrations (11th, 22nd and 37th). That is, using the ZPs starting from the 4th term of defocus and ending with the spherical aberration term, a

total of 8, 19 and 34 terms of modes are included. And compare the restoration effects of the two methods of the same atmospheric turbulence strength.

4. Results

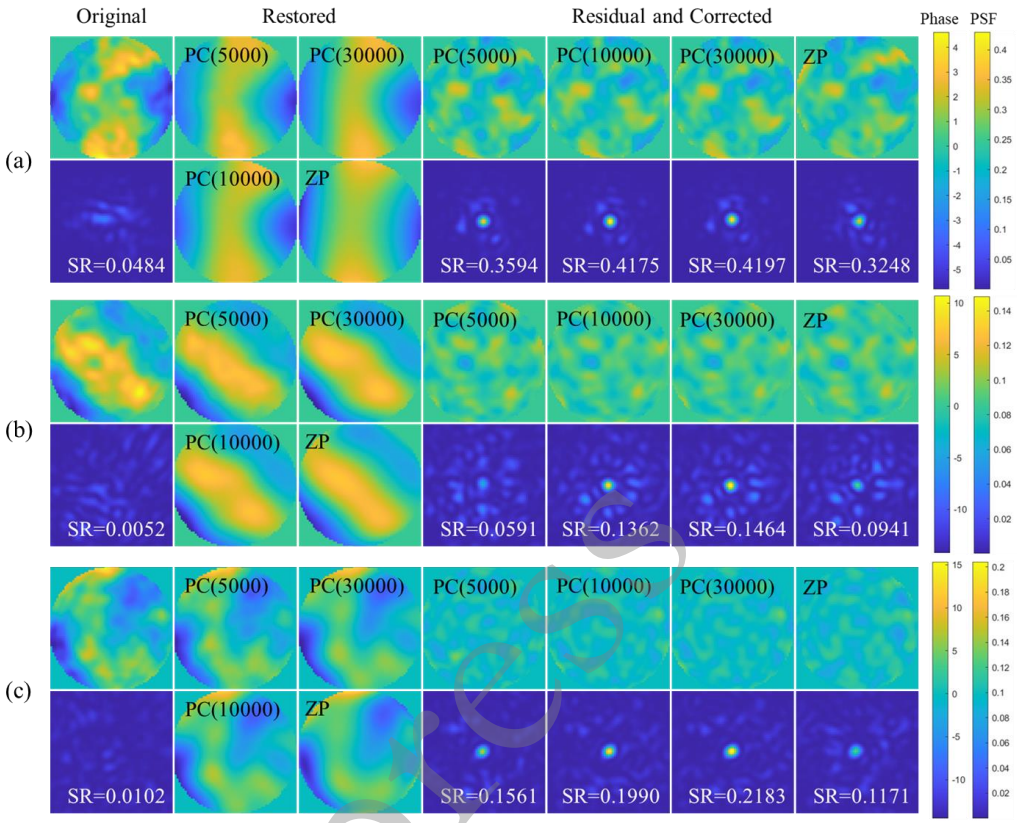

Fig. 1. Examples of restoration by ZPs vs PCs obtained from different sizes of sample spaces

(a) $D/r_0 = 8$, using first 8 terms; (b) $D/r_0 = 16$, using first 19 terms;

(c) $D/r_0 = 24$, using first 34 terms.

图 1 - 不同数据量提取的 PCs 与 ZPs 还原相位畸变的效果示例

(a) $D/r_0=8$，使用 8 项模式；(b) $D/r_0=16$，使用 19 项模式；(c) $D/r_0=24$，使用 34 项模式

Fig.1 shows the restoration effects of equivalent terms of ZPs and PCs obtained from *A*-5000, *A*-10000, and *A*-30000 datasets. In order to provide a comprehensive demonstration of the restoration effects, we took test sets of $D/r_0=8$, 16, and 24, and restoration was performed using first 8, 19, and 34 terms PCs and ZPs, respectively. The terms employed are started with 4th ZP: defocus, and end with the Zernike primary, secondary and tertiary spherical aberrations (11th, 22nd and 37th). Fig. 1 shows the positive correlation between the amount of original data and the restoration effect of PCs. When 5000 sets of original phase data are used, the advantage of PCs may not be obvious yet: the corrected SR obtained using 8 terms of PCs obtained from 5000 sets of original data in graph (a) is only slightly higher than SR obtained by ZPs; as the amount of original data increases, the accuracy of PCs improves, and the gap with ZPs gradually widens: when using the PCs generated from 30000 sets of original data, the corrected spot is clear and bright in graph (c), where the turbulence is stronger and the SR can reach 0.2183. At which point the SR after restoration using PCs obtained from 5000 sets is 0.1561, while the SR after restoration using equivalent terms of ZPs is only 0.1171. It can be seen that when the turbulence is strong, the advantage of PCs is more significant, showing that PCs are stable and consistent, and can adapt to different environments.

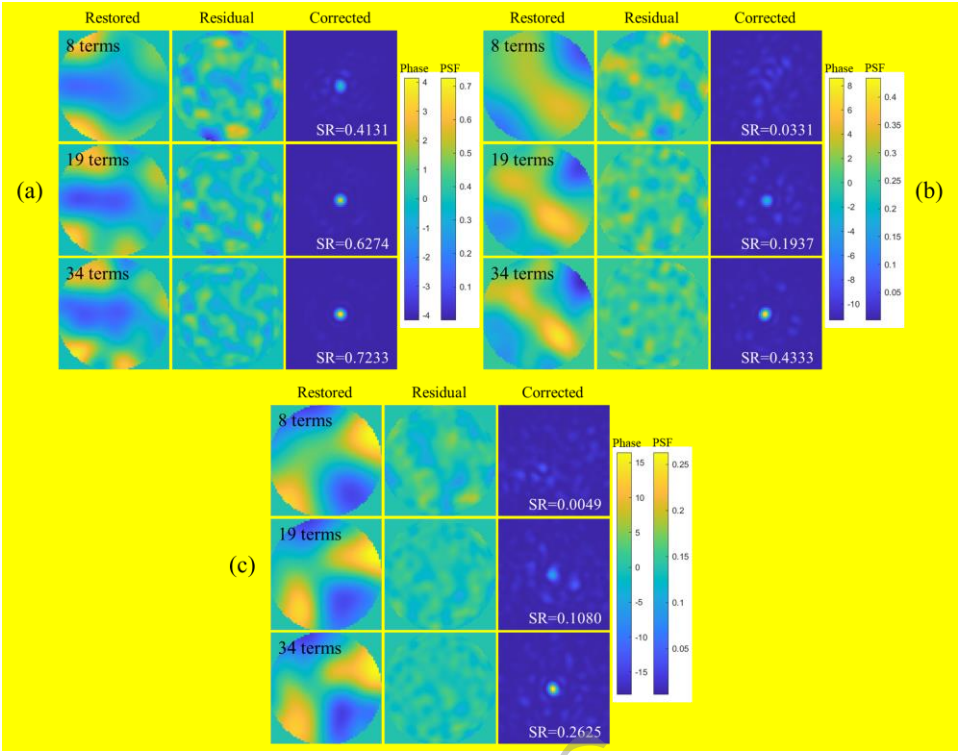

Fig. 2. Examples of restoration by 8, 19 and 34 PCs
(a) $D/r_0 = 8$; (b) $D/r_0 = 16$; (c) $D/r_0 = 24$

图 2 – 相同湍流强度下使用不同数量 PCs 模式的还原效果示例

Furthermore, Fig. 2 shows the effect of using different numbers of terms of PCs to restore the same phase aberration under the same turbulence strength. The PCs used were extracted from 30000 sets of original data. Combined with Fig. 1, it can be seen that when the turbulence strength is weak, the phase aberration can be effectively restored using only 8 terms of PCs, and the corrected SR reaches 0.4131, which further indicates that the PCs can effectively extract the main features of the phase aberrations; when the turbulence strength is medium, the aberration can be effectively restored using 19 terms of PCs, and in the case of strong turbulence, the phase aberration can still be stably restored using 34 terms of PCs, and the corrected SR is about 0.2. This result again shows that PCs have the robustness to manage different turbulent environments and may be more suitable than ZPs

for working in challenging environments such as strong turbulence.

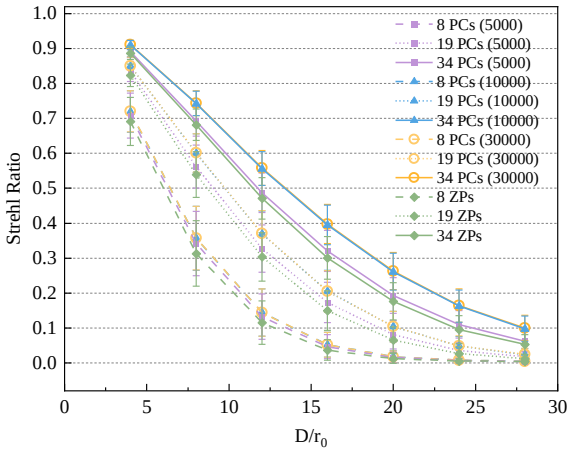

Fig. 3. Mean Strehl ratio after phase aberration restoration by ZPs vs PCs obtained from different sizes of sample spaces

图 3 – 使用不同数据量提取的 PCs 与 ZPs 还原相位畸变后均值 SR 对比

Fig.3 further explores the mean SR after restoring phase aberrations at different turbulence strengths using equivalent terms of ZPs and PCs that were extracted from different sample spaces. It can be seen that the PCs obtained from the 30000 sets of original phase data is the most effective in restoring the phase aberrations. This is because the larger the data volume, the broader the model. It's worth noting that PCs from 10000 sets (blue triangular scatter lines) and 30000 sets (orange circle scatter lines) almost overlap in Fig.3, suggesting a limited impact of size of sample space. If the original data already covers enough phase information, adding more sampled data won't improve the accuracy of PCs much, but will just make the data more redundant, which will hinder the rapid deployment of models in real-world applications. This provides an important basis for model optimization of PCs in practical applications.

Although increasing the size of the sample space can improve the accuracy of PCs, it can also increase the burden of computational and time costs. In the actual model deployment, it’s desirable to obtain the most accurate PCs of the phase aberrations caused by the local atmospheric turbulence with the shortest possible sampling time. The D/r_0 sampling interval is increased from 1 in *A*-space to 10 in *B*-space to analyze the impact of the sampling interval on the accuracy of the PCs. Fig.4 shows the

comparison of the restoration for the same phase aberrations by PCs obtained from *A*-5000 and *B*-5000. It is clear that the restoration by PCs obtained from the *B*-5000 with larger sampling intervals are much better than those from the *A*-5000.

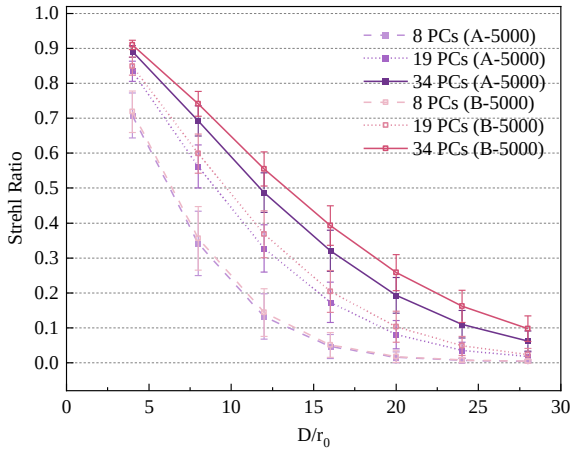

Fig. 4. Mean Strehl ratio after phase aberration restoration by PCs obtained from *A*-5000 vs. *B*-5000

图 4 – 使用 *A*-5000 与 *B*-5000 提取的 PCs 还原相位畸变后均值 SR 对比

Table 1 - Mean Strehl Ratio after phase restoration by PCs obtained from *B*-5000 vs *A*-30000 (The first row 4-28 indicates the D/r_0 of test sets)

表 1 – 使用 B-5000 与 A-30000 提取的 PCs 还原相位畸变后均值 SR 对比（第一排 4~28 表示测试集的 D/r_0）

Terms	D/r_0 / N	4	8	12	16	20	24	28
8	5000	0.719	0.3563	0.1437	0.0515	0.0177	0.0072	0.0046
	30000	0.7204	0.3577	0.1439	0.0521	0.0176	0.0073	0.0047
19	5000	0.8496	0.5989	0.368	0.204	0.103	0.0482	0.0235
	30000	0.8505	0.6011	0.3702	0.2049	0.1041	0.0488	0.024
34	5000	0.9101	0.7412	0.5547	0.3925	0.2582	0.1616	0.0978
	30000	0.9108	0.7436	0.5582	0.3978	0.2636	0.1644	0.1002

Tab-1 shows the comparison of the restoration by PCs from *B*-5000 and *A*-30000, and it can be seen that when the sampling interval is increased, the accuracy of the PCs obtained from only 5000 sets of sampled data can be comparable to that obtained from 30000 sets of sampled data.

This is because when the sampling interval is increased, the number of sampling

points is reduced and the size of the sample space corresponding to a single sampling point is increased, so that dataset can contain more different information in a wider range. Therefore, when it is necessary to deploy the PCs model quickly for restoration, the size of the sample space can be reduced and the sampling interval can be increased to ensure the generalization and robustness of the model while reducing the redundancy of the data.

Fig.5 is the examples of restoration by PCs generated from the *B*-5000 and ZPs of equivalent terms. The graph (c) in Fig.5 reflects that in challenging environments, such as strong turbulence, PCs are more effective than ZPs for restoration of phase aberration. Both using the first 34 terms, the SR of the PSF after restoration by PCs has reached 0.1585, which can meet the requirements of engineering applications. While at this time, the SR of the PSF after restoration by ZPs is only 0.02, and comparing with the SR of the original spot PSF, which is 0.007, the effect of the ZP for restoration is almost negligible. It can be seen that PCs perform better, which is consistent with the previous Fig.1 and Fig.3, demonstrating the stability of PCs again.

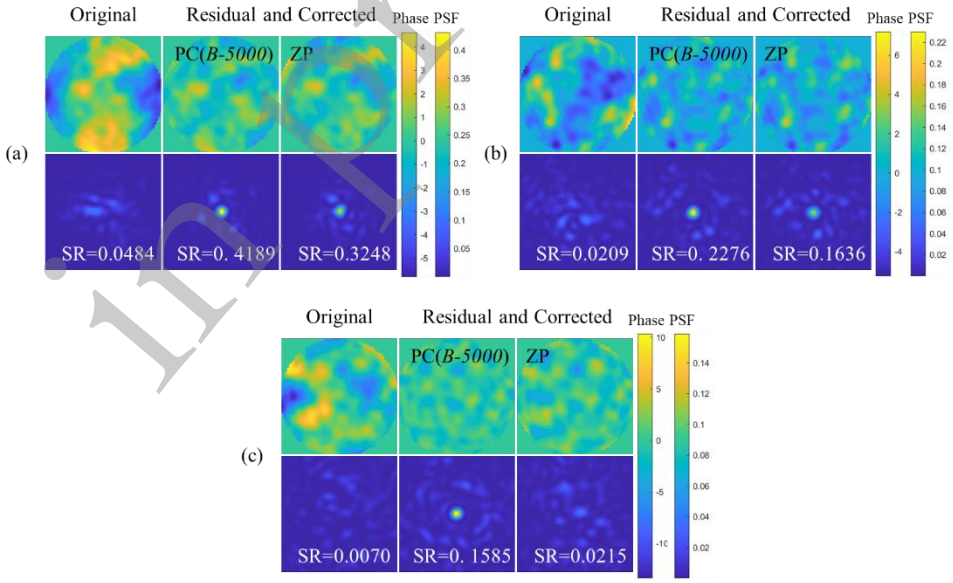

Fig. 5. Examples of restoration of phase aberrations by the equivalent terms of ZPs vs PCs obtained from B-5000

(a) $D/r_0 = 8$, using first 8 terms; (b) $D/r_0 = 16$, using first 19 terms; (c) $D/r_0 = 24$, using first 34 terms.

图 5 – 使用相等数量的 PCs（从 B-5000 提取）和 ZPs 模式还原相位畸变效果示例

(a) $D/r_0=8$，使用 8 项模式；(b) $D/r_0=16$，使用 19 项模式；(c) $D/r_0=24$，使用 34 项模式

5. Conclusion

In this paper, the factors affecting the restoration accuracy of PCs, mainly the size of sample space and D/r_0 sampling interval, are discussed in depth on the basis of characterizing phase aberrations by PCs. The results show that the more the sample data, the higher the accuracy of the PCs and the better the adaptability in restoring phase aberrations in different environments. However, when the sample space contains enough phase information, the increase in the sampled data no longer improves the accuracy of the PCs but results in data waste. When the model needs to be deployed quickly, the generalization and robustness of PCs can be ensured by appropriately reducing the size of sample space and increasing the sampling interval.

In general, our work reveals that PCA method evidently outperforms traditional ZPs across varying atmospheric turbulence strength, especially in challenging situations such as strong turbulence, indicating that PCA method can be served as a better alternative in restoring the phase aberrations induced by atmospheric turbulence. These findings may help to reduce data dimensionality, i.e., using PCs of phase aberrations with less terms than traditional ZPs, which is useful for improving model-based and deep learning based adaptive optics correction.

References:

[1] Mahajan V N. Aberrations of diffracted wave fields. I. Optical imaging[J]. JOSA A, 2000, 17(12): 2216-2222.

[2] Angel J R P, Wizinowich P, Lloyd-Hart M, et al. Adaptive optics for array telescopes using neural-network techniques[J]. Nature, 1990, 348(6298): 221-224.

[3] Sandler D G, Barrett T K, Palmer D A, et al. Use of a neural network to control an adaptive optics system for an astronomical telescope[J]. Nature, 1991, 351(6324): 300-302.

[4] Jia P, Ma M, Cai D, et al. Compressive Shack–Hartmann wavefront sensor based on deep neural networks[J]. Monthly Notices of the Royal Astronomical Society, 2021, 503(3): 3194-3203.

[5] Hartlieb S, Wang Z, Rüdinger A, et al. Large dynamic range Shack–Hartmann wavefront sensor based on holographic multipoint generation and pattern correlation[J]. Optical Engineering, 2024, 63(2): 024107-024107.

[6] Volkov M V, Bogachev V A, Starikov F A, et al. Numerical study of dynamic adaptive phase correction of radiation turbulent distortions and estimation of their frequency bandwidth with a Shack–Hartmann wavefront sensor[J]. Atmospheric and oceanic optics, 2022, 35(3): 250-257.

[7] Li P, Tang F, Wang X. Relationship between shear ratio and reconstruction accuracy in lateral shearing interferometry[J]. Optical engineering, 2020, 59(3): 034113-034113.

[8] SONG Jinwei, MIN Junwei, YUAN Xun, et al. Four-wave transverse shear interferometric quantitative phase imaging based on two-dimensional Ranch phase grating [J]. Journal of Photonics, 2022, 51 (11): 220-229.

宋金伟,闵俊伟,袁勋,等. 基于二维朗奇相位光栅的四波横向剪切干涉定量相位成像 [J]. 光子学报, 2022, 51 (11): 220-229.

[9] Sinha A, Lee J, Li S, et al. Lensless computational imaging through deep learning[J]. Optica, 2017, 4(9): 1117-1125.

[10] Chen M, Jin X, Li S, et al. Compensation of turbulence-induced wavefront aberration with convolutional neural networks for FSO systems[J]. Chinese Optics Letters, 2021, 19(11): 110601.

[11] Lohani S, Glasser R T. Turbulence correction with artificial neural networks[J]. Optics letters, 2018, 43(11): 2611-2614.

[12] Guo Y, Zhong L, Min L, et al. Adaptive optics based on machine learning: a review[J]. Opto-Electronic Advances, 2022, 5(7): 200082-1-200082-20.

[13] Paine S W, Fienup J R. Machine learning for improved image-based wavefront sensing[J]. Optics letters, 2018, 43(6): 1235-1238.

[14] Nishizaki Y, Valdivia M, Horisaki R, et al. Deep learning wavefront sensing[J]. Optics express, 2019, 27(1): 240-251.

[15] Ge X, Zhu L, Gao Z, et al. Experimental demonstration of wavefront reconstruction and correction techniques for variable targets based on distorted grating and deep learning[J]. Optics Express, 2024, 32(10): 17775-17792.

[16] Qitao W, Shoufeng T, Youhui X. On simulation and verification of the atmospheric turbulent phase screen with Zernike polynomials[J]. Infrared and Laser Engineering, 2013, 42(7): 1907-1911.

[17] Siddik A B, Sandoval S, Voelz D, et al. Deep learning estimation of modified zernike coefficients and recovery of point spread functions in turbulence[J]. Optics Express, 2023, 31(14): 22903-22913.

[18] Lv H, Fu S, Zhang C, et al. Speckle noise reduction of multi-frame optical coherence tomography data using multi-linear principal component analysis[J]. Optics Express, 2018, 26(9): 11804-11818.

[19] Zhang Q, Xiao G, Lan Y, et al. Atmospheric turbulence detection by PCA approach[J]. Aerospace Systems, 2019, 2: 15-20.

[20] Terreri A, Pedichini F, Del Moro D, et al. Neural networks and PCA coefficients to identify and correct aberrations in adaptive optics[J]. Astronomy & Astrophysics, 2022, 666: A70.

[21] Schmidt J D. Numerical simulation of optical wave propagation with examples in MATLAB[J]. (No Title), 2010.

[22] Noll R J. Zernike polynomials and atmospheric turbulence[J]. JOsA, 1976, 66(3): 207-211.

[23] Lane R G, Glindemann A, Dainty J C. Simulation of a Kolmogorov phase screen[J]. Waves in random media, 1992, 2(3): 209.

Author biographies:

Jiangpuzhen Wang (1998-), PhD student, University of Science and Technology of China (USTC). Her research interests are on phase aberrations correction due to atmospheric turbulence. E-mail: puzhen98@mail.ustc.edu.cn.